JJMIE

Volume 3, Number 2, June. 2009
ISSN 1995-6665
Pages 131- 140

Jordan Journal of Mechanical and Industrial Engineering

Investigation of the Mach Number Effects on Fluid-to-Fluid Interaction in an Unsteady Ejector with a Radial-Flow Diffuser

A.K. Ababneh[a,*], C.A. Garris[b], A.M. Jawarneh[a], H. Tlilan[a]

[a] *Department of Mechanical Engineering, Hashemite University, Zarqa, Jordan 11134*

[b] *Department of Mechanical Engineering, George Washington University, Washington DC, USA*

Abstract

The concept of fluid-to-fluid direct interaction whereby energy can be transferred among the interacting fluids was demonstrated and shown to be conceivable in non-steady ejectors. Unlike steady ejectors, the mechanism responsible for the energy transfer is reversible and thus higher efficiencies are expected. Of interest is to investigate the effects of Mach numbers on the performance of non-steady ejectors with radial-flow diffusers. The radial-flow ejectors usually lead to higher-pressure ratios with fewer stages. The Mach number of the primary fluid flow emerging out of the free-spinning rotor is considered an important factor among various parameters that affects the process of energy transfer. Specifically, the flow field is investigated at two Mach numbers 2.5 and 3.0 utilizing rectangular short-length supersonic nozzles for accelerating the primary fluid. Also the effects of increasing the total pressure of the primary fluid on the flow field are investigated. The results are compared with earlier investigation at Mach number 2.0, which showed significant enhancement in energy transfer with increase in Mach number. Fundamental to the enhancement of these devices performance relies on the management of the flow field in such a way to minimize entropy production. Numerical analysis utilizing a package of computational fluid dynamics was used for the investigation.

Keywords: Non-Steady Ejector; Fluid-to-Fluid Interaction; Pressure Exchange; Supersonic Flow; Radial-Flow Diffuser

Nomenclature *

B	Body force per unit mass, (N/kg)
c_v	Specific heat at constant volume, (J/kg-K)
c_p	Specific heat at constant pressure, (J/kg-K)
$\ddot{e}$	Deformation tensor, (1/s)
E	Total energy of system per unit mass and it includes internal and kinetic, (J/kg)
Es	The ratio of energy recieved by the secondary fluid relative to case M=2.0
F	Viscous surface forces of a fluid particle, (N/kg)
h	Static enthalpy, (J/kg)
h_o	Total enthalpy, (J/kg)
H	Height of rectangular supersonic nozzle at exit, (mm)
$\ddot{I}$	Identity strain tesor (1/s)
LHS	Left Hand Side
L_N	Length of the rectangular supersonic nozzle; from throat to exit plane, (mm)
L_{th}	Height of the supersonic nozzle at throat
mm	millimeter
p	Static pressure, (N/m^2)
$P_{o,ri}$	Total inlet pressure of the primary fluid, (N/m^2)
$P_{o,si}$	Total inlet pressure of the secondary fluid, (N/m^2)
$P_{o,so}$	Total outlet pressure of the secondary fluid, (N/m^2)
PEE	Pressure Exchange Ejector
q	Heat transfer flux, (W/m^2)
RHS	Right Hand Side
$\ddot{T}$	Stress tensor -with dots on top- which includes viscous and pressure, (N/m^2)
T_o	Total temperature, (K)
$T_{o,si}$	Total inlet temperature for the secondary fluid, (K)
$T_{o,so}$	Total outlet temperature for the secondary fluid, (K)
u	Fluid particle velocity in a non-inertial frame of reference, (m/s)
V	Fluid particle velocity, (m/s)
W	Depth of the rectangular supersonic nozzle and is constant throughout, (mm)
ϕ	Gravity potential, (N-m/kg)
μ	Dynamic viscosity of fluid, ($N\text{-}s/m^2$)
ρ	Density of fluid, (kg/m^3)
$\ddot{\tau}$	Viscous stress tensor, (N/m^2)
Ω	Angular velocity, (1/s)

1. Introduction

Therein lies a mechanism that regulates the energy flow between two directly interacting fluid-to-fluid which

* Corresponding author. *ababneh_hu@hu.edu.jo*.

potentially could be an optimal means for the energy transfer from high energetic fluid to a low energetic one. For this mechanism to come about the flow field must be unsteady. Non-steady ejectors have been utilized whereby this mechanism of energy transfer can take effect. The concept of non-steady ejector was introduced by Foa [1-3] and has since then been investigated by many researchers. The bulk of the work until the mid 1990s was focused on thrust augmentation where the theme was to induce larger mass flow rates for enhancing propulsion thrust; e.g., see [4-7]. Furthermore, this early research work was concerned with the primary fluid being accelerated to less than sonic speeds.

Fundamentally, this mechanism responsible for the energy transfer is related to pressure forces and it becomes apparent when the energy equation is expressed in the following differential form,

$$\frac{Dh_o}{Dt} = \frac{-1}{\rho}\nabla \cdot \bar{q} + \frac{1}{\rho}\,\bar{f} \cdot \bar{V} + \frac{1}{\rho}\frac{\partial p}{\partial t} \qquad (1)$$

The left hand side of the equaiton represents the net rate of energy acquired by a fluid particle as it traverses an unsteady flow field, the first term on the right hand side is the energy transfer via heat transfer mode, the second is the energy transfer via the shear forces & turbulence mixing and the third is the energy transfer through the work of pressure forces. The later mode of energy transfer is often refered to as "pressure exchange" by researchers working in the field. The essence of the work of pressure forces that it is reversible in nature. In the classical ejectors, or as referred to steady ejectors, the unsteady term vanishes simply because the flow is steady hence for their operation they rely on the work of shear forces and turbulent mixing, highly non-reversible processes.

The non-steady ejectors, or sometimes are called pressure exchange ejectors, are considered to be an extension of the steady ejectors since they share several mechanical design features; i.e., primary fluid inlet ducting, secondary fluid inlet ducting, interaction region, a diffuser and more importantly they are known for their mechanical simplicity. However, a unique aspect of the non-steady ejectors is that they contain a frictionless free-spinning rotor whereby the flow is made non-steady with respect to an absolute frame of reference.

Beginning with the mid 1990s Garris [8-11] introduced the concept of utilizing supersonic nozzles to accelerate the primary fluid to supersonic speeds in the hope of achieving higher compression ratio of the secondary fluid for applications other than thrust augmentation as for example in the case of refrigeration and power augmentation. Soon experimental work for validation of concepts followed. Initial efforts, at the George Washington University, were made at building and testing a radial-flow non-steady ejector because of the potential application of this type. Basically, the radial-flow ejector consists of a free-spinning rotor embodied with as many supersonic rectangular nozzles as desired; The primary fluid is permitted to enter through the supersonic nozzles. The region where the two fluids are allowed to come in contact is confined between two plates where the flow is predominantly radial. Further description of the testing apparatus and concepts can be found in related work cited above.

Unforeseeably, the experimental work was halted because of mechanical difficulties; e.g., failures in thrust bearings, seals, development of instabilities and vibration in the set-up. Meaningful data could not be collected from the experimental work. Since then research activities have focused on numerical simulation to resolve the flow field regarding the radial-flow ejectors.

Numerical investigation was a step forward in keeping progress regarding the radial-flow non-steady ejector as well as other configuration [12-13]. The studies revealed in the case of subsonic flow fundamental features of the flow pattern whereby results showed vividly the two fluids remained discernable and separable throughout the ejector and at the same time energy was being transferred between the two interacting fluids. This is a distinct aspect to pressure exchange ejectors and a fundamental difference from steady ejectors whereby in the later mixing and turbulence are the mechanisms by which they energize the secondary fluid; i.e., in the steady ejectors the two interacting fluids emerge completely mixed. Therefore, higher performance levels for energizing secondary fluids when utilizing pressure exchange mechanism are perceivable. However, in the case of supersonic flows, the analyses revealed that the flow is predominantly unstable, hence the uniformity and quality of the flow was not observed to be as in the case of subsonic flow. Specifically, the flow field in the case of subsonic was observed to be steady in a reference frame attached to the rotating rotor while in the case of supersonic flow the two fluids tended to mix. The unsteadiness of the flow observed from the numerical results is likely the cause for the vibration encountered during the actual experimental work. The investigations were limited to subsonic flow and one case of supersonic flow at Mach number 2.0 with nozzles positioned at two spin angles 10^o and 20^o [14].

Undoubtedly, attaining higher levels of performance will necessitate going higher with Mach numbers as well as resolving the flow field instabilities. Therefore, in this paper the effects on the flow field of higher Mach numbers; i.e., 2.5 and 3.0, and that due to higher total pressure are investigated. Higher Mach numbers are achieved utilizing short-length rectangular supersonic nozzles with their profiles were generated using the method of characteristics. The base-line level for the boundary conditions; i.e., the total pressures, is that where the primary and secondary fluids are met at the matched condition which corresponds to the onset of the interaction between the two fluids, this in turn is governed by the secondary inlet total pressure. The total pressure of the primary fluid is then increased beyond that level to examine its effects on the flow field and performance. The matched condition is where the static pressures of the two fluids are the same, which results in perfect expansion of the primary fluid and also starts the interaction with no shocks.

Although the underlying objective is to gain further understanding of the various aspects of the energy transfer mechanism between the interacting fluids, in addition there are technical advantages of studying non-steady ejectors. For example, as has been repeatedly elucidated by various researchers working in the field that these devices are well

suited for steam refrigeration and hence environmental negative effects due to the use of the prevailing refrigerant nowadays can be significantly reduced if steam refrigeration becomes competitive alternative. Second, steam can be generated utilizing waste heat, which is abundant in automotive that utilizes internal combustion engines, therefore less of fossil fuel may be burned which otherwise needed to drive typical air-conditioning compressors.

2. Geometry and Model Construction

The ejector basically consists of three main parts as depicted in Figure 1: one, is the free spinning rotor; two, is the inlet ducting for the secondary fluid; and three, is the radial-flow diffuser. The free spinning rotor is the inner portion of the ejector, which includes the rectangular supersonic nozzles and spins on an axis aligned with the z-axis. It is exploded in Figure 1-d where in addition to the spin rotor half of the inlet ducting of the secondary fluid is shown. The inlet ducting of the secondary fluid is that portion where only the secondary fluid is present and it is seen to resemble an inner racing of a bearing in Figure 1-b; also half of it is seen in Figure 1-d. The radial-flow diffuser is the region where the two fluids come in physical contact and exchange energy. A segment of the diffuser is depicted in Figure 1-c. The length of the diffuser L_d (91.2 mm) is maintained constant for the two cases (M=2.5 and M=3.0) and is chosen of the same length as that in the case of M=2.0. The overall model geometry is based on the actual model that was attempted for the experimental study [10], however, the radial diffuser was modified to lessen the severity on the supersonic flow as was recommended [14] so that unnecessary shocks generation are avoided. The rectangular supersonic nozzles (total of 8) are positioned at a spin angle of 10^o from the meridian plane. The spin angle is the parameter that permits the rotor to spin.

As mentioned for accelerating the primary fluid two sizes of short-length rectangular supersonic nozzles are used in this study. The profiles for these nozzles were generated utilizing the method of characteristics [15,16]. The nozzles share the same cross-sectional area at the throat as that of M=2.0 [14]. The pertinent dimensions of the nozzles are given in Table 1. The nozzles were verified separately under stationary conditions for the purpose of ensuring the generation of the desired Mach numbers; e.g., 2.5, and 3.0, using ideal air isentropic analyses. These simulations showed satisfactory results as evident in Figure 2, which depicts the Mach number and total pressure variations along the distance in the stream wise direction. Also included in Figure 2 the results pertaining to the case M=2.0.

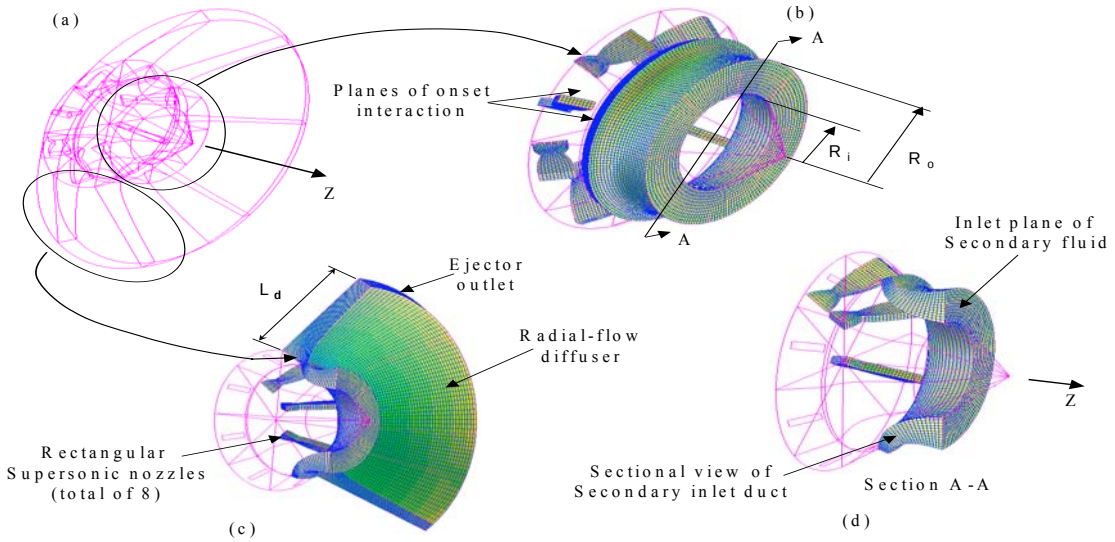

Figure 1. Non-steady flow ejector: (a) wire frame of the ejector; (b) inlet ducting of the secondary fluid and also is shown the rectangular supersonic nozzles; (c) radial-flow diffuser; and (d) wire frame of the rotor and a sectional view of the inlet ducting for the secondary fluid.

Table 1. Dimensions of the rectangular supersonic nozzles; each nozzle is specified by its design Mack No.

Mach No.	L_{th} (mm)	L_N (mm)	H (mm)	W (mm)
2.0	5.2	12.5	8.7	4.8
2.5	5.2	25.1	14.8	4.8
3.0	5.2	49.0	25.2	4.8

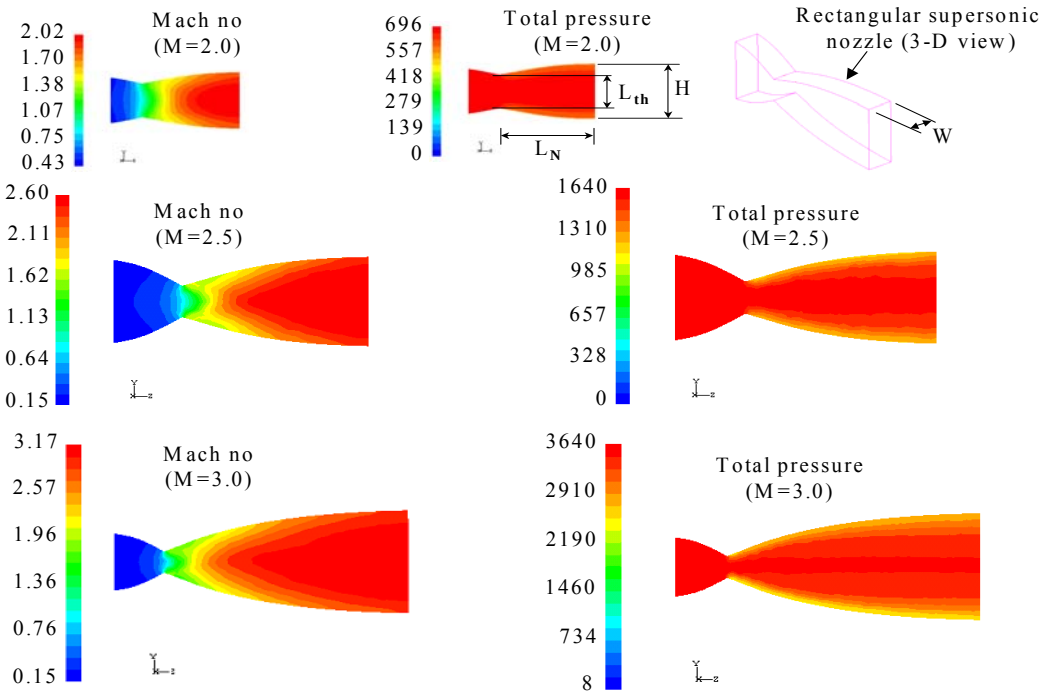

Figure 2. Mach number and total pressure variation in the stream wise direction in the three rectangular supersonic nozzles; Mach No =2.0, 2.5, 3.0.(Total pressure is in gage kPa).

3. Governing Equations and Solution Validations

3.1. Governing Equations

Because the aim of this paper is to investigate the effects of the Mach number and the total pressure of the primary fluid on the effectiveness of the pressure exchange mechanism; i.e., the third term in the right hand side of equation (1), the flow field is taken to be laminar, thus ignoring turbulant mixing. The governing principles are the basic equations of fluid motion; i.e., the continuity, momentum and energy equations [15,17]. The differential form of the continuity equation is

$$\frac{\partial \rho}{\partial t} + \nabla \cdot \rho \vec{V} = 0 \tag{2}$$

The momentum principle is that the rate of change of linear momentum for an enclosed region fixed in space is equal to the sum of forces acting on the region, which is expressed in a differential form as

$$\rho \frac{D\vec{V}}{Dt} = -\nabla p + \rho \vec{B} + \nabla \cdot \ddot{\tau} \tag{3}$$

Assuming the fluids being of Newtonian type along with the Stokes hypothesis the viscous stress tensor is expressed as

$$\ddot{\tau} = -\tfrac{2}{3}\mu \ddot{I} + 2\mu \ddot{e} \tag{4}$$

Where $\ddot{e}$ is the deformation tensor and μ is the fluid dynamic viscosity.

For the energy equation it is expressed as

$$\rho \frac{DE}{Dt} = \nabla \cdot \ddot{T} \cdot \vec{V} + \nabla \cdot \vec{q} \tag{5}$$

Where E is the sum of the internal and kinetic energies and $\ddot{T}$ is the stress tensor; with double dots on top. Potential energies is normally neglected in the case of gases. The working fluid is ideal air for both primary and secondary, hence the internal energy and enthalpy are expressed as

$$u = c_v T \quad and \quad h = c_p T \tag{6}$$

where T is the temperature. The equation of state for the ideal air is used to complete the system of equations.

3.2. Solution and Boundary Conditions

In the absolute frame of reference the interaction of the primary fluid with the secondary is time depedent. The problem, however, is treated with respect to a frame of reference attached to the rotor. In this non-inertial coordinate frame of reference the continuity and energy equations are unaffectedby by the coordinate transformation whereas the momentum equation is re-casted to account for the coordinate transformation, since Newton's Law of motion equates applied forces to acceleration in an inertial frame of reference.

As a result of the coordinate transformation there are two terms that appear; namely, the centriputal and Coriolis accelerations. The centriputal forces can be considered as an additional body force and hence they are added to the gravity potential.

The viscous dissipation term is unaffected by the coordinate transformation and hence the momentum equation becomes

$$\rho\left[\frac{D\vec{u}}{Dt}+2\vec{\Omega}\times\vec{u}\right]=-\nabla p+\rho\vec{F}+\rho\nabla\phi \qquad (7)$$

The second term in the LHS is the Coriolis forces, **F** represnets the viscous surface forces, ϕ is the gravity potential and Ω is the angular velocity. The velocity **u** is the relative velocity in the rotating frame of reference [18].

The angular speed of the rotor is based on the ideal free spinning speed of the rotor. Under the assumption of no applied external torque and in the absence of friction effects the fluid emerges from the nozzles with an exit velocity along the meridian plane for each nozzle. However, this speed is numerically fine tuned based on the energy conservation. The variation from the ideal speed is mainly due to the effects of nozzles three-dimensionality [8].

The boundary conditions include specifying the total pressure at the inelt ductings for the primary and secondary fluids. Because the primary is the energetic fluid its mass flow rate and velocity are known at the inelt while the masss flow rate of the secondary fluid is determined from the solution which results from the induction action. At the outlet of the ejector the static pressure is specified. Because the ejector performance is not known ahead of time and the two fluids have non-uniform conditions in the interaction region, the specification of the outlet static pressure was tangibly involved. An iterative approach was adopted where an efficiency of the ejector was first assumed and then the static pressure based on perfect mixture of the two fluids was computed. The solid walls provided the remaining boundary condition for the flow confinement. The current investigation considers mainly inviscid fluid and hence the walls provide the slip condition. In some cases, viscous effects were included to account for their action on the secondanry fluid, but the walls effects is turned off by considering slip condition. Thus, the normal component to the wall of the relative velocity with no seepage vanishes. Mathematically,

$$\left(\vec{u}-\vec{V}_b\right)\cdot\vec{n}_n=0 \qquad (8)$$

where **n** is the normal vector of the walls and $\mathbf{V}_b$ is the boundary velocity relative to the inertial frame of reference.

The optimal operating point for non-steady ejectors where entropy production is anticipated to be minimized has been recognized to be at the matched point [8,9] whereby the static pressures of the two interacting fluids at the onset of interaction are the same. The matched point specifies the baseline conditions; i.e., for the primary total pressure.

The numerical method is based on the Method of Finite Volume Finite Difference whereby the domain is subdivided into grid points with each point is surrounded by its control volume in a manner that is non-overlapping with the neighboring grid points' control volumes. Piecewise functions can be used as the simplest forms for expressing the variations of the dependent variables between the grid points. The discritization in this manner expresses the conservation of the dependent variables over the grids' control volumes just as the differential forms of the governing equations for the infinitesimal control volume. The implication is that mass, momentum, and energy equations are exactly satisfied; and not just in the limiting sense when the number of grid points becomes large [19].

The solutions were obtained utilizing the Computational Fluid Dynamics (CFD) package FLUENT-v6.2.16, which is a sophisticated analytical and a state of the art package and has been developed over the years. The package in addition to predicting fluid flows behavior it handles problems that involve heat transfer, mass transfer and as well as chemical reaction. The package also has found application in industry such as in Aerospace/Defense, Appliances, Automotive, Biomedical, etc.

3.3. Validation of The Solution

Because of the lack of experimental data to compare with the validation of the numerical solutions concerning the flow filed for pressure exchange ejectors with radial-flow diffuser, the validation is made in two ways. One is to demonstrate that the numerical technique is capable of resolving the flow field of a similar problem that involves the same mechanism of energy transfer but has an analytical solution. Second, is to verify that the numerical solution is convergent and consistent.

The shock tube, which has an analytical solution, has been utilized as a test case for the verification of the numerical procedure concerning the problem described herein. The unsteady events of the flow field in a shock tube begin at the onset of membrane breakup whereby energy flows from the energetic fluid to the low-energetic one and is shown to be governed by equation (1) [15-16]. The analytical solution however, is simplified by considering ideal fluids and neglecting the effects of thermal transfer thus the only term left on the right hand side of equation (1) is the unsteady pressure term, which is the mechanism that is being investigated herein. Figure 3 shows the pressure and velocity behind the traveling shock, moving to the right, in the tube after the membrane is broken up which was placed at position –12.5 mm. The initial temperature and pressure for the primary and secondary fluids were set at 500 K & 500 kPa, gage, and 330 K & 0 kPa, gage, respectively. Both fluids were chosen as ideal compressible air. From the analytical solution the pressure and velocity behind the traveling shock are 153.0kPa, gage and 259.3 m/s, which compares very well with the solution. The CFD method also did capture details of the phenomenon involved by revealing the expansion nature behind it (i.e., to the left where it s being gradual) and compression aspect ahead of it.

The convergence of the numerical solution has been demonstrated throughout this work and is evident from the results, which are presented in section 4. The consistency of the solutions was demonstrated by considering smaller mesh sizes and showing that the solutions are non-significantly different. Also to be noted the numerical procedure has shown satisfactory results when verifying

the flow in the supersonic nozzles (Figure 2), however, the procedure in this case was of a steady nature.

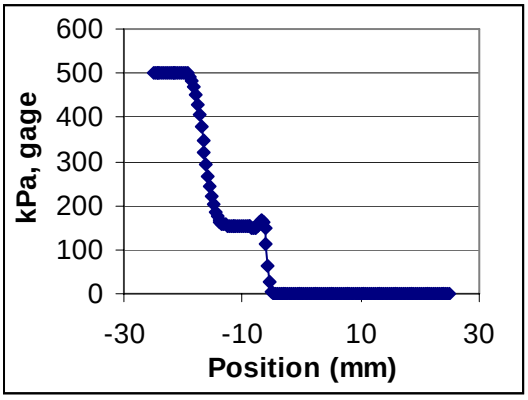

(a)

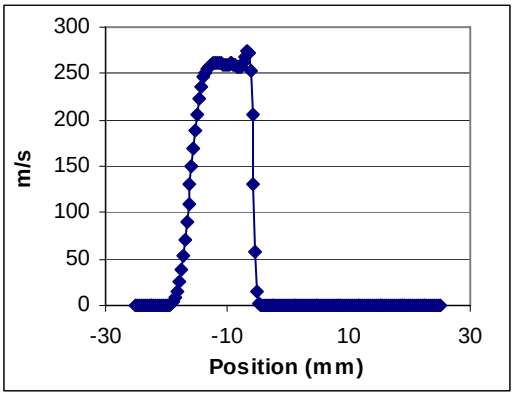

(b)

Figure 3. (a),(b). Pressure and velocity distribution along the shock tube .

The convergence of the numerical solution has been demonstrated throughout this work and is evident from the results, which are presented in section 4. The consistency of the solutions was demonstrated by considering smaller mesh sizes and showing that the solutions are non-significantly different. Also to be noted the numerical procedure has shown satisfactory results when verifying the flow in the supersonic nozzles (Figure 2), however, the procedure in this case was of a steady nature.

4. Results and Discussions

As dictated by equastion (1) the total enthalpy of a fluid particle traversing a non-steady flow field will change accordingly. This fact is demonstrated in Figure. 4 which shows the total temperature distribution in an r-z and r-θ planes of the ejector (Figure. 1). Recall that for an ideal gas the total enthalpies and temperatures differ by a constant. Prior to the onset of the interaction the total temperature of the secondary fluid remains constant T_o = 300 K since it entirely occupies the ejector's secondary nozzle. The secondary nozzle is a convergant ducting that is located in the opposite side that contains the primary supersonic nozzles. Down stream of the onset plane of interaction the total temperature for the secondary fluid is seen to increase continuously at the expense of the primary fluid. The two fluids can be distinguished from each other by examining the r-θ planes (identified at the locations z = 0.035, 0.045, 0.050) whereby the primary fluid is seen to have the higher T_o as compared to the secondary fluid. Further the primary fluid is observed to be localized in small elliptical areas since it leaves the rectangular supersonic nozzles at smaller areas while the secondary fluid fills the areas in between the primary jets; there are a total of eight primary jets corresponding to the number of the supersonic nozzles.

The unstability nature of the flow is evident in Figure 4 where the uniformity and quality of the flow is not well preserved as seen in the case of subsonic flow [14]; observe how the primary fluid is smearing as it progresses in the ejector; e.g., moving in the rθ planes identified with z = 0.035, z = 0.045 and z = 0.05. However, it is clear that the two fluids are still separable a feature is highly desirable in these technologies sepecially in the case of having dissimilar fluids. The primary jets were observed to oscillate causing the flow to be unbstable. The oscillation is likely caused by a system of waves reflections and interactions in the diffuser which eventually leads to distorting the flow field pattern. The non-stability of the flow and the oscillation of the primary jets are, most probably, the cause for the actual vibration developed during the actual experimental attempts. Therefore, a step forward in these technologies will invlove the flow management for yielding well behaved flow.

Consequent to the energy gained by the secondary fluid is that it is enabled to flow through the ejector by entering at the secondary inlet ducting, where its total pressure is set at 0 Pa gage, and overcoming a static pressure boundary 2kPa gage set at the outlet of the ejector. What is important however is that the secondary fluid is induced into the ejector at high speeds as evident in Figure 5 where it is seen that the velocity is approximately reaching 300 m/s at the secondary throat. Eventually, the total pressure at the outlet of the ejector is the measure of the useful work transferred to the secondary fluid. In addition, the mass rate of induction of the secondary fluid is required to compute the rate of energy transferred. Figure 6 shows the induction mass flow rate of the secondary fluid, which is caused, by the action of the primary fluid on the secondary. The Figure also reveals the non-stability nature of the flow field; nonetheless, the overall flow is remaining stable by yielding a time-average value of nearly 0.35 kg/sec for the case of Mach no 2.5.

The underlying mechanism is fundamentally different in a pressure exchange ejector than in a steady ejector. In the later the driving force for energizing the secondary flow is due to turbulence mixing and shear stresses hence the flow quickly tends to uniformity in all aspects and consequently the two fluids, primary and secondary, become essentially indiscernibile.

To the contrary in pressure exchange ejector when the flow is well maintained and managed by carefull design, only energy is allowed to flow from the primary to the secondary via the pressure forces that act at the inerfacial surfaces between the two fluids and eventually the two fluids emerge out of the ejector intact and seperable. These facts are still confirmed as depicted in Figure 4 even thoguh the flow was not maintained as orderly as in the caseyofhsubsonicgflow[14].

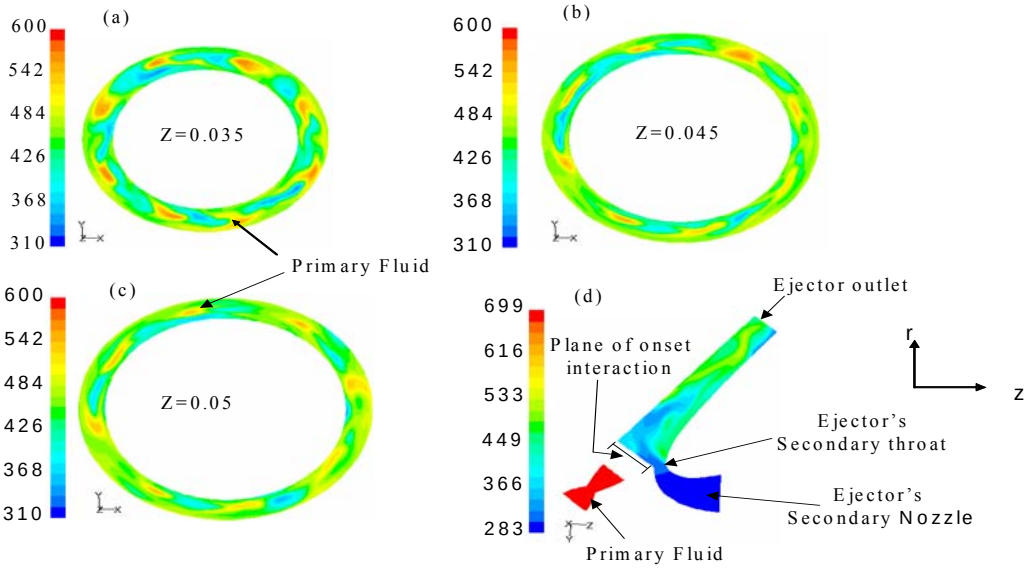

Figure 4. Total temperature variation M=2.5 in different planes of the ejector: a, b, and c are r-θ planes at z=0.035, 0.045, and 0.050, while d is an r-z plane.

The unstability nature of the flow is evident in Figure 4 where the uniformity and quality of the flow is not well preserved as seen in the case of subsonic flow [14]; observe how the primary fluid is smearing as it progresses in the ejector; e.g., moving in the rθ planes identified with z=0.035, z=0.045 and z=0.05. However, it is clear that the two fluids are still separable a feature is highly desirable in these technologies sepecially in the case of having dissimilar fluids. The primary jets were observed to oscillate causing the flow to be unbstable. The oscillation is likely caused by a system of waves reflections and interactions in the diffuser which eventually leads to distorting the flow field pattern. The non-stability of the flow and the oscillation of the primary jets are, most probably, the cause for the actual vibration developed during the actual experimental attempts. Therefore, a step forward in these technologies will invlove the flow management for yielding well behaved flow.

Consequent to the energy gained by the secondary fluid is that it is enabled to flow through the ejector by entering at the secondary inlet ducting, where its total pressure is set at 0 Pa gage, and overcoming a static pressure boundary 2kPa gage set at the outlet of the ejector.

What is important however is that the secondary fluid is induced into the ejector at high speeds as evident in Figure 5 where it is seen that the velocity is approximately reaching 300 m/s at the secondary throat. Eventually, the total pressure at the outlet of the ejector is the measure of the useful work transferred to the secondary fluid. In addition, the mass rate of induction of the secondary fluid is required to compute the rate of energy transferred. Figure 6 shows the induction mass flow rate of the secondary fluid, which is caused, by the action of the primary fluid on the secondary. The Figure also reveals the non-stability nature of the flow field; nonetheless, the overall flow is remaining stable by yielding a time-average value of nearly 0.35 kg/sec for the case of Mach no 2.5.

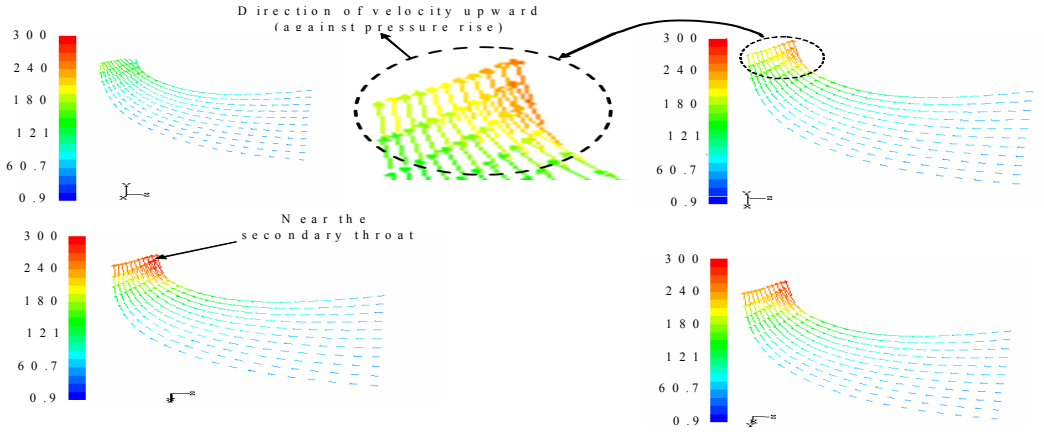

Figure 5. Secondary fluid velocity in the ejector's secondary inlet in different r-z planes.

  - Volume 3, Number 2 (ISSN 1995-6665)

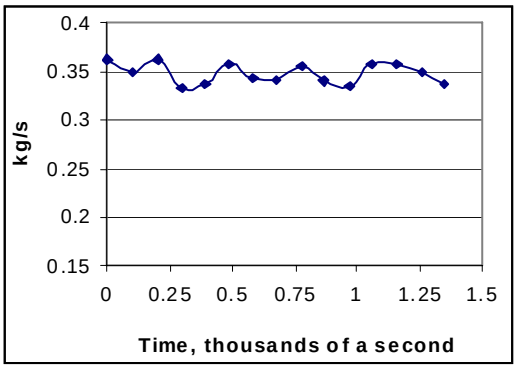

Figure 6. Mass flow rate of the secondary fluid induction. Mach no = 2.5.

The underlying mechanism is fundamentally different in a pressure exchange ejector than in a steady ejector. In the later the driving force for energizing the secondary flow is due to turbulence mixing and shear stresses hence the flow quickly tends to uniformity in all aspects and consequently the two fluids, primary and secondary, become essentially indiscernibile. To the contrary in pressure exchange ejector when the flow is well maintained and managed by carefull design, only energy is allowed to flow from the primary to the secondary via the pressure forces that act at the inerfacial surfaces between the two fluids and eventually the two fluids emerge out of the ejector intact and seperable. These facts are still confirmed as depicted in Figure 4 even thoguh the flow was not maintained as orderly as in the case of subsonic flow [14].

Examining Figure 4 closely it is evident that the total enthalpy of the primary is decreasing as the fluid proceeds in the ejector; e.g., compare Figure 4a and c. That is the level of total enthalpy of the primary fluid, which is seen as the red spots, is decreasing in value when moving from rθ planes z=0.035 (Figure 4a) to z=0.045 (Figure 4b) and to z=0.05 (Figure 4c). On the otherhand, the secondary fluid which fills the space between the primary fluid is seen to increase in total enthalpy when moving outward in the planes along the z-axis. In the limit as the diffuser gets larger, it is expected that the total pressures of the two fluids will become identical and hence energy transfer will come to an end; at least in terms of useful work. The total pressure is used to measure the ejector performance since the total temperature includes the effects of irreversibilities such as the rise in static temperature due to the presence of shocks and shear stresses. Therefore, to evaluate the performance of the ejector the mass averaged of the total pressures at the outlet was obtained, see Figure 7 which reveals the variation in the outlet total pressure. Mean averages over a reasonable length of time were used for computing the total pressure to account for flow non-stabilities. The peculiar difference in the two curves at the begining of the simulation time is due to a difference in the initial starting conditions. Table 2 summarizes the results in the form of pressure ratio ($P_{o,so}/P_{o,si}$) gained by the secondary fluid versus that of the primary fluid $P_{o,ri}/P_{o,si}$.

The cases presented in Table 2, except for case 3, are for the matched conditions; i.e., the static pressures of the two fluids are equal at the onset of the interaction. The amount of energy Es, last column, received by the secondary fluid is seen to increase with Mach number. The Es is the ratio of energy recieved by the secondary fluid relative to case 1 and it is related to the product of the compression ratio and the mass flow rate. Note also that for choked conditions the mass rate is proportional to the total pressure and inversely to the square root of the total temperature. Because increasing Mach number while maintaining matched conditions implies that the total pressure of the fluid must increase, case number 3 was generated to isolate the effects of Mach number on the performance. Specifically, the inlet total pressure equal to that of case number 4, total pressure for Mach no 3.0, was used with the case of Mach no 2.5. The increase in performance seen in case 4 over that of case 3 is mainly due to the Mach number effects, which clearly reveals its superiority in terms of energy transfer over case 3. One reason for this behavior is that at the matched conditions there are no developed shocks at the onset of interaction and hence less of entropy production is generated in the flow which eventually leads to higher performance.

Table 2. Summary of Mach number effects on ejector performance.

Case no.	Mach No	$P_{o,ri}/P_{so,i}$	$P_{o,so}/P_{o,si}$	m_s/m_p	Es
1	2.0	4.13	1.11	1.71	1.0
2	2.5	9.03	1.10	1.28	1.5
3*	2.5	19.4	1.36	0.68	5.7
4	3.0	19.4	1.35	0.81	6.6

* Total pressure is at higher level than that at the matched conditions.

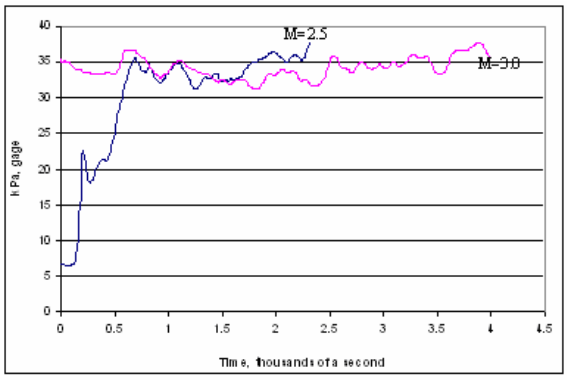

Figure 7. Effects of Mach number on ejector performance; total pressure ratio 19.4 for both cases (M=2.5 and M=3.0).

The increase in the level of compression ratio of the secondary fluid with the total pressure has lead to evaluating the ejector at primary pressure levels higher than the ideally matched conditions Figure 8. The matched conditions are expected to yield best performance since entropy production due to shocks are expected to be least; in the case of ideal fluids entropy production should be zero if no shocks are developed in the diffuser. Nevertheless, in real applications where higher compression ratio for the secondary fluid are desired it may be necessary to run ejector beyond the matched conditions simply because higher Mach number requires longer supersonic nozzles (see Table 1.0) as well as higher velocities which might be more involved in terms of

entropy production due to stronger shocks in the diffuser. The results from the these simulations with pressures higher than the match condition are summarized in Table 3 for the case with M = 3.0. Similar trend is expected with the other cases. In these simulations, it was also observed that the quality of the flow improved with the increase in the primary total pressure by showing less flow reversals and non-stability.

The implication of this is that the diffuser may have been starved of fluid at lower pressures. It is to be noted that the primary mass flow rate m_p increases with total pressure thus leading to the mass ratio of the secondary m_s to the primary to decrease.

Table 3. Effects of primary pressure on the ejector performance. Mach no = 3.0.

$P_{o,ri}/P_{o,si}$	$P_{o,so}/P_{o,si}$	m_s/m_p
19.4	1.35	0.81
20.1	1.41	0.75
30.0	1.78	0.53
40.0	2.38	0.39
50.0	3.02	0.31

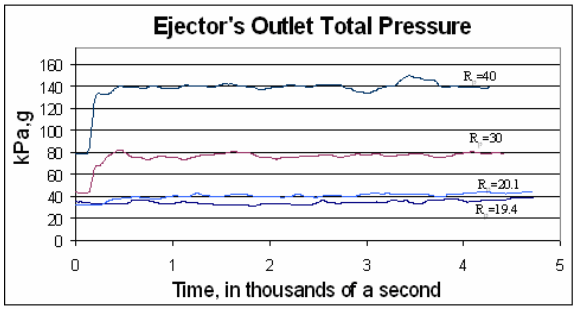

Figure 8. Variation of outlet total pressure at Mach no = 3.0; curves identified with the ratio in total pressure of primary to secondary ($R_p=P_{o,ri}/P_{o,si}$).

5. Conclusions

The flow field of a non-steady ejector with a radial-flow diffuser was investigated at Mach numbers; i.e., M=2.5 and 3.0, as well as with total pressure of the primary fluid that are higher than those at the matched conditions. Results have confirmed anticipated trend whereby optimal performance of non-steady ejectors are achieved when they are operated at matched conditions as was demonstrated in Table 2 with cases 3 and 4. It was observed that the increase of the Mach number resulted in an increase in the amount of energy transfer to the secondary fluid. However, with the increase in Mach number longer supersonic nozzles are required as well as the flow field in the diffuser will be more susceptible for stronger shocks due to the higher velocities. Thus, from practical engineering point it may be necessary to run these devices at total pressures higher than their optimal design point; i.e., higher than that of the matched conditions, but with lesser Mach numbers. As evident from Table 3, higher compression ratio of the secondary fluid can be readily obtained with the increase in the primary total pressure.

The flow behavior was also observed to be of less severe in terms of non-stabilities and flow reversals with higher total pressures, however still showing non-stabilities. This quality of the flow is a critical area that must be resolved to improve the performance of these devices. The improvement in the flow pattern with the increase in total pressure is likely related to the diffuser of being less starved of fluid. Nonetheless, additional studies must be carried out to systematically produce higher flow qualities.

The results also showed clearly the two fluids are still discernable and separable throughout the flow field and most importantly near the ejector's outlet; i.e., after energy is transferred to the secondary fluid.

This is a distinguishing feature of non-steady ejectors especially if the fluids are dissimilar.

References

[1] Foa JV. New method of energy exchange between flows and some of its applications. Technical Report No. TR-AE-5509: Rennselaer Polytechnic Institute; December 1955.

[2] Foa JV. Elements of flight propulsion. John Wiley & Son; 1960.

[3] Foa JV, Garris CA. Cryptosteady modes of direct fluid-fluid energy exchange. Chapter in ASME Book AD-7; 1984.

[4] S.M. Amin, C.A. Garris, "An experimental investigation of a non-steady flow thrust augment". AIAA/ASME/SAE/ASEE Joint Propulsion Conference, Paper No.AIAA-95-2802, July 1995.

[5] Avellone G. Theorectical and experimental investigation of the direct exchange of mechanical energy between two fluids. Grumman Research Dept. Memorandum RM 365; June 1967.

[6] Costopoulos T. A wide-jet strip analysis of crypto steady-flow thrust augmenters Parts 1 and 2. Technical Report No. TR-UTA-772: George Washington University; March 1977.

[7] K.H. Hohenemser, J.L. Porter, "Contribution to the theory of rotary-jet flow induction". J. Aircraft, Vol. 3, No. 4, July 1966, 339-346.

[8] C.A. Garris, W.J. Hong, "Radial-flow pressure exchange ejector". ASME Proceeding of the Third International Symposium on Pumping Machinery, Vancouver, Canada, June 1997.

[9] Garris CA. Pressure exchange ejector and refrigeration apparatus and method. US Patent No. 5,647,221; July 1997.

[10] C.A. Garris, W.J. Hong, C.M. Mavriplis, J. Shipman, "A new thermally driven refrigeration system with environmental benefits". Intersociety Engineering Conference on Energy Conversion, Colorado Springs, Co, August 2-6,1998.

[11] Garris CA. Pressure exchange compressor-expander and method of use. US Patent No. 6,434,943 B1; August 2002.

[12] W.J. Hong, K. Al-Hussan, H. Zhang, C.A. Garris, "A novel thermally driven rotor-vane/pressure-exchange ejector refrigeration system with environmental benefits and energy efficiency". International Conference on Efficiency, Costs, Optimization, Simulations and Environmental Impact of Energy Systems, Berlin, Germany, July 3-5, 2002.

[13] K. Al-Hussan, C.A. Garris, "Non-steady three dimensional flow field analysis in supersonic flow induction". ASME International Fluids Engineering Summer Conference, Montreal, Canada, July 14-18, 2002.

[14] Ababneh AK. Investigation of fluid to fluid interaction in a radial-flow pressure exchange ejector. PhD Dissertation, George Washington University; 2003.

[15] Anderson JD. Modern compressible flow with historical perspective. McGraw-Hill Inc.; 1990.

[16] Saad MA. Compressible fluid flow. Prentice Hall, Inc.; 1993.

[17] Aris R. Vector tensor and the basic equations of fluid mechanics. Prentice Hall; 1962.

[18] Pedlosky J. Geophysical fluid dynamics. 2nd ed, Springer-Verlag; 1987.

[19] Pantankar SV. Numerical heat transfer and fluid flow. Hemisphere Publishing Corporation; 1980.